

OPTICAL MEASUREMENT, COMPARISON AND SIGNALING OF LARGE FREE FORM SURFACES

Tiago Loureiro Figaro da Costa Pinto, tlp@joinville.ufsc.br

Universidade Federal de Santa Catarina, Centro de Engenharia da Mobilidade.

Christian Kohler, chr.kohler@gmail.com

University of Stuttgart, Institut für Technische Optik.

Armando Albertazzi Gonçalves Junior, albertazzi@labmetro.ufsc.br

Universidade Federal de Santa Catarina, Departamento de Engenharia Mecânica.

***Abstract.** Many surfaces, such as ship hulls or wind turbines are typical examples of free form surfaces and optical measuring systems are increasingly used for the measurement of these surfaces. A portable optical system, capable of measuring free form surfaces over large areas, comparing them with reference surfaces and locally project color maps onto the surface to signal parameters of interest, was developed within this work. The system merges passive and active stereo vision. Algorithms perform the calculation intrinsically structured point clouds into a single regular mesh, allowing the use of any number of cameras and structured light projectors. The calibration of the projector, as an inverted camera, allows calculating and designing a color map, to signalize surface features, helping the dimensional control of the object and monitoring of machining. Experimental evaluations, using different kinds of geometric patterns and free form surfaces demonstrate the feasibility and the advantages of using the proposed methods.*

***Keywords:** geometric control, stereo vision, fringe projection, free form surface.*

1. INTRODUCTION

Many surfaces, such as ship hulls, fairing of automobiles and rotors of water or wind turbines are typical examples of free-form surfaces. Like any pieces produced by industry, parts that contain free-form surfaces should also be measured, to ensure that the product function is performed satisfactorily. Optical metrology systems are increasingly used for the measurement of free-form surfaces. Measurements by optical principles have several advantages: (a) contact free measuring, (b) high speed measurements, where millions of points can be measured within seconds, (c) high portability and (d) measurement uncertainties that are comparable to contact measurement systems (Pinto, 2010).

A portable optical system, capable of measuring free-form surfaces over large areas to compare them with reference surfaces and locally project color maps on the surface to signal parameters of interest, was developed within this work. The system merges passive and active stereo vision. Circular targets are used to concatenate three-dimensional point clouds in a global coordinate system. Algorithms perform the calculation of these intrinsically structured point clouds into a single regular mesh, allowing the use of any number of cameras and a structured light projector. These algorithms also allow measuring the points in several coordinates systems and points of interest in predefined directions. The calibration of the projector, as an inverted camera, allows calculating and designing a color map, to signalize surface features of interest, helping the dimensional control of objects and monitoring of machining.

Experimental evaluations, using different kinds of geometric patterns and free form surfaces demonstrate the feasibility and the advantages of using the proposed methods.

2. FREE-FORM SURFACE MEASUREMENT

The measurement of free-form surfaces is usually done by measurement of three-dimensional points, using a mechanical probing system or by optical techniques. In the following are some optical techniques and variations that can be used for the measurement of free-form surfaces.

2.1. Close range photogrammetry

Close range photogrammetry consists of methods for acquisition and interpretation of images to determine the shape and location of an object from two or more images taken from different angles. The technique converts the two-dimensional information contained in images, in three-dimensional information of the object. For the calculation of three-dimensional points, the principle of triangulation is used, which determines lines connecting points on the object of its various projections of the images acquired. These lines are constructed from the pinhole camera model, dominant in computer vision for 3D scene reconstruction based on image acquisition (Luhmann, 2003)(Daniilidis and Klette, 2006).

The pinhole model considers that the projection of an image on a screen through a lens can be described by projecting 3D points in a plane through a central point called the center of projection. For any point \mathbf{M} in 3D space, its representation in the image \mathbf{m} is located where the line joining \mathbf{M} with the center of projection \mathbf{C} intersects the image plane π . The projection $\mathbf{m} = (x.w, y.w, w)^T$ of a 3D point $\mathbf{M} = (X, Y, Z, 1)^T$ in the plane π can be described by the equation (Hartley and Zisserman, 2003)(Zhang, 1998)(Zhang, 1999)(Heikkilä and Silvén, 1997):

$$\mathbf{m} = \mathbf{P}\mathbf{M} = \mathbf{A}[\mathbf{R} \ \mathbf{t}]\mathbf{M} \quad (1)$$

The projection matrix \mathbf{P} is a 3x4 matrix containing a combination of extrinsic (\mathbf{R}, \mathbf{t}) and intrinsic (\mathbf{A}) parameters.

This model does not include distortions introduced by imperfections of the lenses used, which can be quite significant. An usual model for the correction of radial and tangential distortion is mapping the distorted coordinates, which are captured by cameras, for the corrected coordinates (Moumen *et al*, 2003)(Weng *et al*, 1992) (Heikkilä and Silvén, 1997). The final 3D coordinates of the object can be calculated through a simultaneous optimization of these data, in a technique known as bundle adjustment (Triggs *et al*, 2000).

In practice, several images are taken at different positions and rotations of the camera, with a high degree of convergence, coverage and redundancy in relation to the object. Length standards in the same scene are used to perform the measurement as scale and for the self-calibration of the camera. For the determination of the measurement points coded and uncoded targets are placed strategically (Lima, 2006)(Remondino and Fraser, 2006)(Rautenberg and Wiggenghagen, 2002) (Raguse and Wiggenghagen, 2003).

2.2. Stereo vision

Stereo vision is a method for the three-dimensional reconstruction of a scene from corresponding points by triangulation with two cameras, which can be considered a special case of photogrammetry (Kanatani *et al*, 2008). In this case, the intrinsic camera parameters and the relative position between the cameras are not changed during the measurement, thus the calibration parameters are fixed, allowing to calibrate the measurement system as a preliminary step to measurement (Stivanello, 2008) (Sünderhauf and Prötzler, 2006).

To perform the triangulation and determine the three dimensional position of a point it is necessary to determine its corresponding position in each of the two images. The epipolar geometry describes the geometric relationship between two independent images of the observed scene. It is depending only on the calibration parameters, and can be used to facilitate the determination of corresponding or homologous points, in images (Hartley and Zisserman, 2003).

One of the constraints imposed by epipolar geometry, is that a 3D point which is projected onto a point \mathbf{m} in a camera must lie on on a epipolar line in other camera image (Stivanello, 2008) (Fantin *et al*, 2007) (Hartley and Zisserman, 2003). Accordingly the search for a homologous point is restricted to a straight line. From the pinhole model, the previously collected calibration data (by methods described in (Zhang, 1998) (Zhang, 1999) (Zhang *et al*, 2006) (Heikkilä and Silvén, 1997)) and the homologous points in each image, it is possible to determine the lines in 3D-space that may contain these points. The intersection of these lines determines the position of point \mathbf{M} in space by the triangulation process.

For the determination of homologous points, without help from other systems or special markers, the scene must contain discrete individual forms that do not form a homogeneous texture (Harris, 1988) and allow the use of simple correlation (Nister *et al*, 2004) (Sünderhauf and Prötzler, 2006). For the measurement of parts that have a homogeneous texture, special markers, such as circular targets or auxiliary systems for the projection of structured light may be used.

2.3. Fringe projection

A technique widely used today to measure surfaces, with high density of points, quickly and automatically, is fringe projection or topogrammetry (Fantin, 1999) (Pinto, 2010). The projection of structured light sequences with phase shifted sinusoidal fringes, allows the measurement of a surface with a high density of points, as it enables the creation of a highly effective signature for identification of homologous points. For phase unwrapping a robust technique using a second sequence of binary images called "Graycode" can be used. It allows an unambiguous determination of the fringe order (Proll, 2004) (Bräuer-Burchardt *et al*, 2008). From the absolute phase maps of the both cameras it is easy to detect fast and precisely homologous points.

A variation of the principle is the phase map profilometer, where for each pixel of the camera a polynomial that correlates the phase value with known positions of a calibration plane is calculated. Later these polynomials are used to determine the 3D positions of points out of measured phase values (Sitnik *et al*, 2002) (Xiaoling, 2005) (Fujigaki and Morimoto, 2008). Another variation is to use a calibrated projector as an inverted camera, from the point of view of geometrical optics. In this case, the homologous points are determined out of the phase map acquired by the camera and the projected phase map (Zhang *et al*, 2006). The triangulation is then performed equal as in the case of two cameras (Zhang, 1998).

To measure large parts, where different positions of the system may be required, some techniques can be used to concatenate the measurements (Kühmstedt et al, 2004): perform a known relative movement between the system and the object (Nerosky, 2001) (Halioua et al, 1985), use the phasogrammetry technique with auxiliary cameras (Kühmstedt et al, 2004), use the aid of photogrammetry (Luhmann, 2003) (Reich, 2000) or the assembling of several measurements using mathematical methods for the alignment and concatenation as Iterative Closest Point (Geron `es, 2007).

2.2. Self-referencing sensors

One type of self-referencing sensor can be the self-referencing laser profilometer, which uses the fusion of two principles in one portable device, stereo vision (passive triangulation) in combination with laser triangulation (active). The self-referencing is referring to the lack of external aids for referencing the overall measurement, allowing a manual handling of the device and offering high flexibility (Hébert, 2001) (Strobl et al, 2009). The stereo vision is used to determine the position of the sensor in relation to the part of interest and laser triangulation to measure the surface by the projection of laser lines onto it. The information of sensor position is used for the concatenation of the data measured at different positions in a single coordinate system.

The stereo vision enables the calculation of 3D coordinates of marks in a single acquisition, and techniques such as ego-motion or visual odometry can be used to calculate the movement of the device between successive acquisitions (Childers and Edwin, 2007) (Tina et al, 1996) (Vassal, et al, 2007) (Majid, 2008). Another approach includes merging data from other sensors such as inertial, which captures the movement of the system in six degrees of freedom (Strobl et al, 2009). Anyway it is possible to perform the self-location of the system using only the 3D measurement data of the makers. These marks or targets should be distributed on the part in a way that at least three must be visible between successive acquisitions (Hébert, 2001) (Khoury, 2006).

The calculation of points on the surface by active triangulation is based on the position of structured laser light captured by the cameras (Nerosky, 2001) (Bonacorsi, 2004). The laser light is usually in the form of a point, line, multiple parallel lines or a pair of concurrent lines (Bonacorsi, 2004)(Geron `es, 2007)(Hébert, 2001). By merging data extracted from the active and passive triangulation sensors, it is possible to reconstruct the shape of the surface.

3. DEVELOPED SYSTEM

The developed system incorporates several features enabling the measurement of large free form surfaces. It also allows comparison between surfaces and signaling the measured surface by the projection of color maps. A complete description of this work can be found in (Pinto, 2010).

The system basically has two measurement modes the stereo-photogrammetric and topogrammetric. The first method measures the three dimensional position of targets, scattered over large areas in relation to a global coordinate system. The other measures in detail a small area of the piece and aligns it with the global coordinate system, into a single regular mesh defined in the XY plane. Both modes use two cameras and a structured light projector.

In stereo-photogrammetric mode, the image acquisition by two cameras allows the reconstruction of three-dimensional target positions into a single global coordinate system. In topogrammetric mode the detailed measurement is performed by the projection and acquisition of structured light projected on the object, allowing the calculation of the absolute phase map and a cloud of dense three-dimensional points (e.g. millions of points). The points are referenced in the global coordinate system, with defined step in X and Y direction.

Two surfaces can be compared using relatively simple algorithms. The data of the two measurements may be calculated in relation to the same coordinate system with the same ordinates and abscissa (X , Y) for each point. To signal characteristics of interest onto the surface, it is possible to calculate and project color encoded maps with the multimedia projector.

3.1. Measurement principle

A new way to make measurements where the measured object points form a regular grid in X - and Y -direction equally spaced points was developed. In contrast to most other systems using fringe projection only one set of phase maps is needed, thus requiring merely the projection of sinusoidal fringe images with one fringe orientation. One main advantage of the technique proposed here is that surface data maybe stored in matrices consisting only of the Z -values. But it requires a special technique for the calculation of the topography points, which will be explained briefly here, a detailed description may be found in (Fantin et al, 2007) (Fantin et al, 2008) (Pinto et al, 2009) (Pinto, 2010).

As a first step a coordinate system is chosen in a convenient manner in the object volume. In principle it does not matter what type of coordinate system is used, e.g. cartesian, cylindrical, spherical or any other type, but for sake of simplicity we will explain the principle using cartesian coordinates. Then a regular grid of object points is defined in the selected coordinate system with the desired point density.

From the phase maps acquired by the cameras and the X and Y coordinates of each point of the regular grid, the search for the according Z coordinate is performed numerically. The value of Z is changed and the resulting 3D point is

projected onto each image plane of the cameras (and projectors) using the projection equations (1) and distortion correction. The phase value corresponding to the calculated camera pixel is determined with subpixel resolution. Theoretically, for the correct value of the Z coordinate the phase value should be equal for all the cameras. In practice, when only two cameras are used, the smallest difference between the phase values must be found. If three or more cameras are used, the Z search stops when the smallest variance between the phase values is found.

Thus, the estimate of the Z coordinate associated with each grid point (X, Y) is determined. The principle can be seen in Fig. 1: for different Z coordinates, for a grid point (X, Y) , their according points in the images of the cameras are calculated.

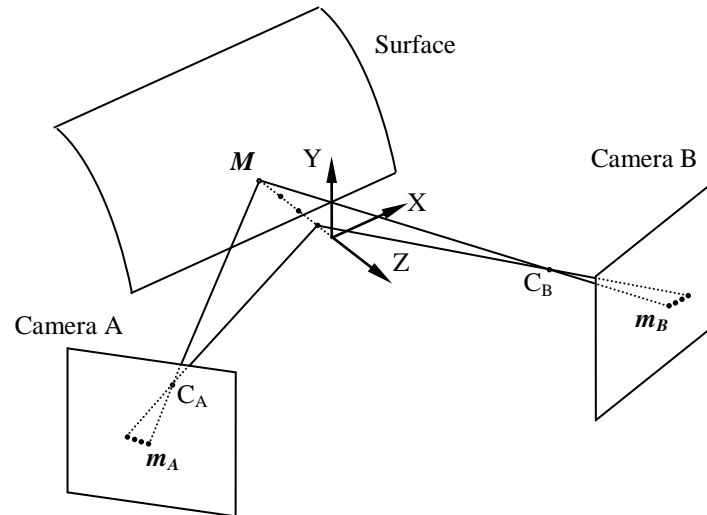


Figure 1: Z coordinate determination for an object point with pre-defined X, Y coordinates.

The algorithm can be summarized as:

1. Define the X, Y coordinates for the grid to be tested;
2. Define the limits of the Z value variation: Z_{min} and Z_{max} ;
3. Set ΔZ dividing the interval between Z_{min} and Z_{max} in n parts;
4. Project each point M formed by the coordinates X, Y and $(Z_{min} + \Delta Z * i)$ with $i = 0, 1, \dots, n$, on the phase maps using equation (1) and inserting the distortion for each camera or projector.
5. Determine the projected point with the smallest difference or variance between the phase values;
6. Set new values for the interval Z_{min}, Z_{max} and the increment ΔZ surrounding the determined Z value with the lowest phase difference;
7. Return to Step 3 and restart the search with the new values of Z_{min}, Z_{max} and ΔZ until the phase difference or variance is sufficiently small;
8. Set the Z coordinate with the lowest phase difference;
9. Return to step 1 to measure another point of the predefined grid, i.e. different X and Y , until the Z values for all points are calculated.

With the techniques exposed in this section, it is possible to perform the measurement of a dense cloud of points (which can be millions of points) in relation to a local coordinate system. The calculated points are organized in a regular grid and are equally distant with a userdefined distance between each other in a predefined coordinate system.

3.2. Concatenation

To perform the concatenation of the measured targets it is necessary to estimate the movement of the system between acquisitions. The technique used to perform the concatenation can be called stereo odometry and is described by Sünderhauf and Prötzler (2006). To determine the correspondence between two consecutive acquisitions of partially overlapping surface areas, an exhaustive search within all possible combinations of always three detected markers is done for each acquisition. The transformation, with the smallest error, is used to transform all surface points of the second acquisition to coordinate system of the first one. All pairs of points whose distance is below a threshold are used for a second iteration for a refining of the transformation. Markers that have a low distance value between them are used to recalculate the markers' positions by means of an averaging. The other markers are added as new ones to the list. Using the concatenated list of markers it is possible to define the global coordinate system of interest.

The concatenation of several acquisitions results in a cloud of points with regular grid extended to all acquisitions. The cloud of points for each acquisition is calculated in relation to the coordinate system of interest defined by the measured and concatenated markers. To perform the measurement, the transformation matrix Gq is used and relates the position q of the measurement coordinate system (MCS) to the global coordinate system (GCS), as illustrated in Fig.2.

Thus, for each camera (or projector) the projection equation is used with the processed extrinsic parameters that the positions of the cameras are expressed in the global coordinate system:

$$m = A \cdot G_q \cdot M \quad \text{with: } G_q = [R \ t]_{cam} \cdot [R \ t]_q \quad (2)$$

M is calculated similarly to that shown in Fig.1, but with projection equation (2), resulting in a single regular mesh, extended to all positions of the system. The boundaries of the grid for each measurement (X_{min} , Y_{min} , X_{max} and Y_{max}) are transformed so that the measured points cover the whole measurement volume in relation to the global coordinate system. For each position q of the system, the same processing is performed for both cameras, as shown in Fig.2, whilst the fixed relationship between the cameras which is included in the previously done calibration is kept constant.

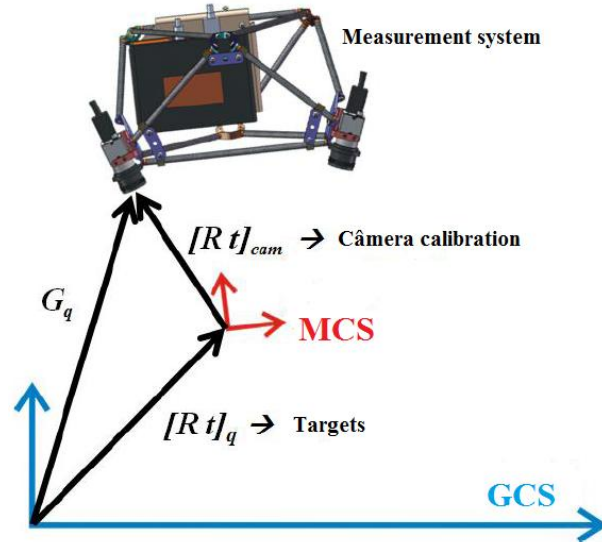


Figure 2. Coordinate systems relations for the concatenation of different clouds of points (Pinto, 2010)

Two clouds of points measured with a partial overlapping of the X and Y coordinates deliver points in the extended regular grid defined by the GCS, with exactly the same X and Y coordinates in the overlapping area. But the Z coordinates of these points are not necessarily equal, due to measurement errors. So as a final step of the calculation of an extended regular grid in the GCS, for all points with same X and Y coordinates in overlapping acquisitions that have more than one Z coordinate a final Z coordinate is calculated by simply averaging the calculated Z values.

3.2. Surface comparison

The regular grid offers a great advantage when two surfaces should be compared, as the comparison results in simply calculating the differences of the Z coordinates for each point of the grid with the same X and Y coordinates. But for this direct comparison, the global coordinate system of the measurement must be chosen carefully because significant errors can be introduced depending on the choice of the coordinate system.

In general, the direct comparison of Z coordinates can be applied for a wide range of applications and is quite simple to implement. Figure 2 shows two different coordinate systems where in (a) the Z direction of the measurement coordinate system is far from the surface normal vector, introducing errors in the comparison. In (b) the Z direction of the measurement coordinate system allows a direct comparison between two measurements not introducing additional errors.

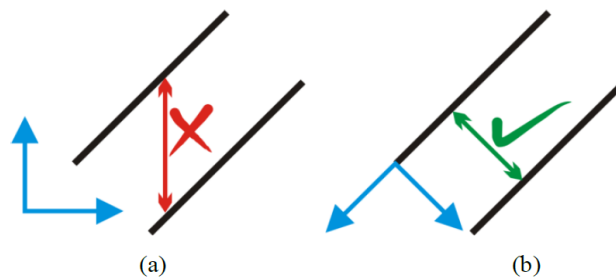


Figure 3. (a) Incorrect and (b) correct coordinate system for the direct comparison of Z coordinates (Pinto, 2010).

As a result, a mesh of differences in Z can be calculated with a low computational effort, unlike conventional comparisons between clouds of points that may require the determination of the correspondence between points on the surfaces before making the comparison.

3.3. Signaling

To assist in locating areas of special interest on a surface, the projection of a color map onto the surface can assist visual inspections or be used for monitoring the progress of a machining process. The criterion for the association of colors to a point on the surface can be for example proportional to the difference from the reference surface, the curvature at each point, the amplitude of the Z coordinate, or other criteria. Also the displaying of contour lines or referencing regions of interest is possible.

For the calculation of the color map and the projection of each colored point onto its physical equivalent point on the surface, the projector is regarded again as an inverted camera. This concept is based on a principle known as Helmholtz reciprocity, where the flow of light can be reversed without altering its intensity properties (Sen *et al*, 2005).

As the calibration parameters of the projector are known, a measured three-dimensional point M can be projected in the image plane of the projector using the projection equations and distortion correction. Each calculated point a color can be associated with some parameter of interest that is related to the correspondent point M on the surface. This color map is a simple two dimensional image, which is projected by the projector.

Of course the calculation of the color map for the projection has to consider the actual shape of the surface, i.e. the shape and position of the 3D surface that should be signaled. Therefore the system has to be in the same position during the measurement and projection of the color map, or markers should be measured to determine the system's position in relation to the global coordinate system and the according coordinate transformation has to be considered in the calculations.

4. EXPERIMENTAL RESULTS

In this chapter, some of the principal results of the research project are described. First, the prototype of the developed measurement system is presented, followed by an evaluation of the system performance based on VDI-VDE guidelines and examples of surface signaling and measured parts are shown.

4.1. Measurement system prototype

One of the aims of the project was the development of a lightweight portable system design. Out of the experiences of preliminary tests an appropriate design integrating two cameras and projector could be found. The structure is designed to minimize manufacturing costs, mass and volume, while maintaining sufficient structural rigidity between the components. Figure 4 (a) shows the mechanical design of the system and its measuring volume and (b) the prototype of the measurement system.

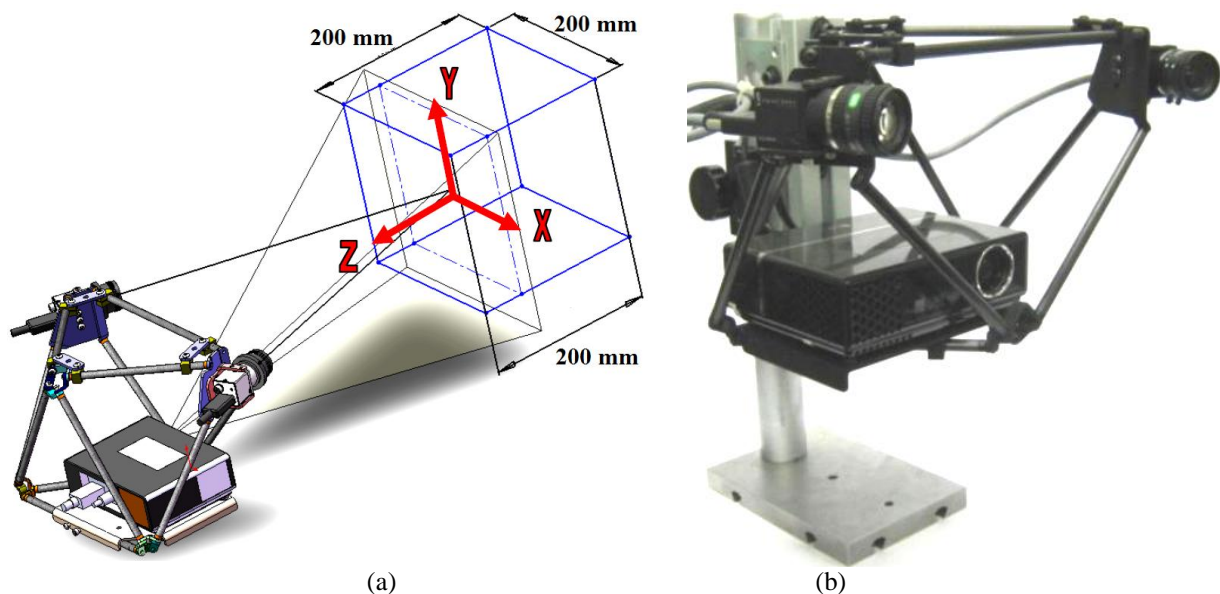


Figure 4. (a) Measurement volume and (b) prototype of the measurement system (Pinto, 2010).

4.2. Evaluation of the system performance

Specific recommendations for evaluation of the performance of optical measurement systems can be found in the (VDI/VDE 2634 Part 1, 2002) and (VDI/VDE 2634 Part 2, 2002) guidelines. The evaluation, which considers only one position of the system (i.e. without concatenation of separate measurements), can be divided into four parameters:

ΔL - length measurement error: a comparison standard should be measured in at least seven positions of the measurement volume. The distances between the markers have to be calculated and compared with calibrated distances. The parameter ΔL is the biggest error of the calculated distances.

RE - Flatness measurement error: a reference plane is measured at predetermined positions. RE is the largest magnitude of distances between the measured points and a plane calculated by a least square regression.

RA - Probing error: is the largest magnitude of the radial deviation between measured points on a sphere and a sphere fitted into the measured point cloud by means of a least square regression, with a variable radius.

SD - Sphere-spacing error: the biggest error found for the distance between the centers of two spheres. The distance between the spheres is determined by a least squares sphere interpolation using a previously calibrated sphere radius.

Figure 5 (a) illustrates the measurement of a linear standard for evaluation of the length measurement error and (b) an image of the standard spheres used for the measurement of probing and sphere spacing error and the result of a measurement with the measured points and the interpolated sphere for probing and sphere-spacing error evaluation. Table 1. shows the main results of the experiments. These data are the maximum errors found, usually in the most unfavorable position for the measurements provided by the VDI-VDE guidelines.

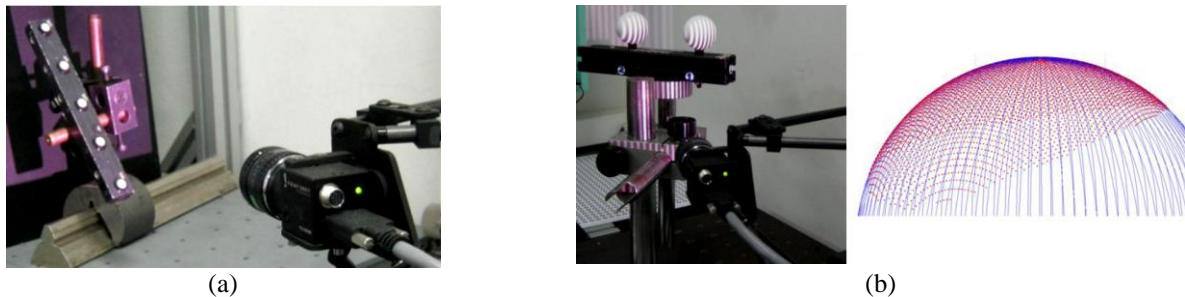


Figure 5. (a) Standard used for evaluating the length measurement error and (b) standard spheres used for the measurement of probing and sphere-spacing error and measured points with fitted sphere (Pinto, 2010).

Table 1. Experimental results for a measurement volume of (200x200x200) mm³.

Parameter	Value [mm]
ΔL - Length measurement error	0,28
RE - Flatness error	0,32
RA - Probing error	0,21
SD - Sphere-spacing error	-0,41

4.4. Surface signaling

A qualitative experiment using a manually constructed free-form surface was realized to show the measurement and projection of a color map associated with the Z coordinates including iso-height-lines. The images in Fig. 6 show (a) the image calculated for projection with colors and iso-height-lines indicating a height difference of 2 mm according to the local object height and (b) a photograph of the signaled part.

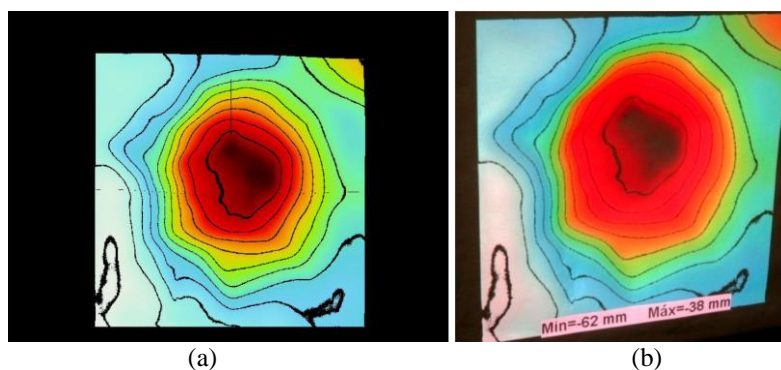


Figure 6. (a) Image calculated for projection and (b) surface signaled for inspection (Pinto, 2010).

No experiments were done to quantitatively evaluate the accuracy of the color projections used for signaling, but the algorithms used to calculate the projected image are the same used for the calculation of the surface Z coordinates explained above and which were validated experimentally. So, we do not expect errors in the indication of surface parameters, larger than the ones determined by the evaluation of the measurement system. The largest errors are expected in the color representing a certain object point as it is calculated by the difference between two surfaces. The lateral position of the point itself, which depends only on the measurement accuracy and the actual position of the measurement system should not exceed the measurement accuracy.

4.5. Measurements examples

Some free form surfaces were measured to illustrate the operation of the system. Figure 7 (a) shows projected sinusoidal fringes used for the measurement of the face of a mannequin (b) shows the resulting cloud of points from a single measurement. Figure 8 (a) shows the image of a cavity filled with welding seams (b) is the result of the surface measurement and (c) local surface height signaled by the projection of a color map. The values for the measurement uncertainty in these examples are no greater than the values found using the VDI-VDE guidelines.

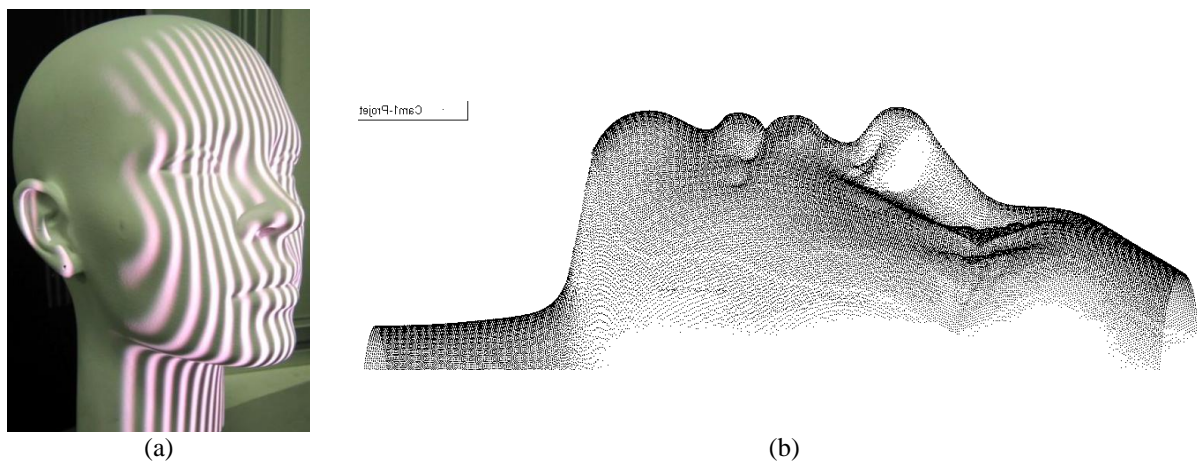


Figure 7. (a) Sinusoidal fringe projected on the mannequin face which is used in the measurement process and (b) resulting point cloud from the measurement (Pinto, 2010).

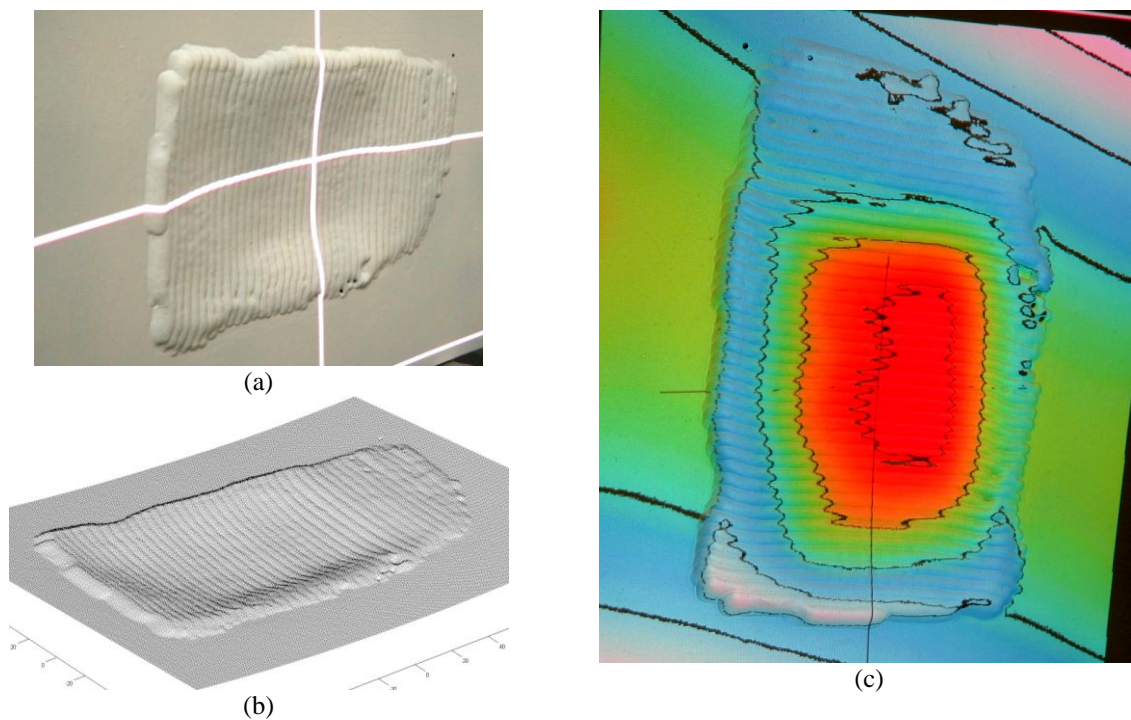


Figure 8. (a) Cavity filled with welding seams (b) measurement result and (c) signaling of the free form surface according to its local height (Pinto, 2010).

5. CONCLUSIONS

We presented in detail the measurement and concatenation algorithms for the measurement of large surfaces in a single regular grid of points. The algorithms and a prototype measurement system were evaluated using the VDI/VDE guidelines and showed their functionality. Using the comparison of surfaces as an example we demonstrated the advantages of the presented system over other previously developed techniques. Future works include the optimization of the algorithms in order to minimize the processing time necessary to view the results.

6. ACKNOWLEDGEMENTS

We would like to thank the Alexander von Humboldt Stiftung by supporting C. Kohler with a Feodor-Lynen scholarship and CNPq, FAPESC and the UFSC for their financial support during the development of this research.

7. REFERENCES

- Bonacorso, N. G., 2004, “Automatização dos processos de medição de superfícies e de deposição por soldagem visando a recuperação de rotores de turbinas hidráulicas de grande porte”, Tese, PósMec, UFSC.
- Bräuer-Burhardt, C. et al, 2008 “Phase Unwrapping in Fringe Projection Systems Using Epipolar Geometry” Springer, ACIVS 2008, LNCS 5259, pp. 422–432.
- Childers; Edwin M.C., 2007 ‘Method and system for obtaining high resolution 3-D images of moving objects by use of sensor fusion’ United States Patent Application 20070064242.
- Daniilidis, K. Klette, R., 2006, “Imaging Beyond the Pinhole Camera” Editora Springer, ISBN-13 978-1-4020-4894-4, 2006.
- Fantin, A. V., 1999, “Medição de formas livres tridimensionais por topogrametria” Dissertação, PósMCI, UFSC.
- Fantin, A. V., et al, 2007, “Efficient mesh oriented algorithm for 3D measurement in multiple camera fringe projection” Optical Metrology 2007, Munique-Alemanha. Proceedings of SPIE, 2007 v. 6616. p. 6616 1B.
- Fantin, A. V., et al, 2008 “Measurement and stitching of regular cloud of points” SPIE 2008, Optical Engineering Applications, 2008, San Diego. Proceedings of SPIE, 2008 v. 7066. p.706607.
- Fantin, A.V *et al*, 2007, “An Efficient Mesh Oriented Algorithm for 3D Measurement in Multiple Camera Fringe Projection” SPIE.
- Fujigaki, M., Morimoto, Y., 2008, “Shape Measurement with Grating Projection Using Whole-Space Tabulation Method”, Journal of JSEM, Vol. 8, No.4, 92-98.
- Geron'es, C. M., 2007, “Hand-held 3D-scanner for large surface registration” Thesis, Universitat de Girona, Espanha.
- Halioua M. *et al*, 1985 “Automated 360° profilometry of 3-D diffuse objects” Applied Optics, vol. 24, no. 14.
- Harris, C., 1988 “A combined edge and corner detector” In Proc. of the Alvey Vision Conference, pg. 147-151.
- Hartley, R., Zisserman, A., 2003, Multiple View Geometry’. Cambridge University Press.
- Hébert P., 2001, “A Self-Referenced Hand-Held Range Sensor” 3-D Digital Imaging and Modeling, Page(s):5 - 12.
- Heikkilä, J., Silvén, O., 1997, “A Four-step Camera Calibration Procedure with Implicit Image Correction” Proceedings of the 1997 Conference on Computer Vision and Pattern Recognition (CVPR '97).
- Kanatani, K., et al, 2008, “Triangulation from two views revisited: Hartley-Sturm vs. optimal correction” Proceedings of the 19th British Machine Vision Conference.
- Khoury, R., 2006, “An Enhanced Positioning Algorithm for a Self-Referencing Hand-Held 3D Sensor” IEEE, Computer and Robot Vision.
- Kühmstedt P. *et al*, 2004 “Phasogrammetric optical 3D-sensor for the measurement of large objects” Optical Metrology in Production Engineering, Proc. of SPIE Vol. 5457.
- Lima, C.R.G., 2006, “Um estudo comparativo de sistema de medições aplicáveis ao controle dimensional de superfícies livres em peças de médio e grande porte” Dissertação, PósMCI, UFSC.
- Luhmann T. N., 2003, “Nahbereichs-photogrammetrie: Grundlagem, Methoden und Anwendungen” Herbert Wichmann Verlag, ISBN 3-87907-398-8.
- Majid Z., 2008, ”Integration of Stereophotogrammetry and Triangulation Based Laser Scanning System for Precise Mapping of Craniofacial Morphology” The International Archives of the Photogrammetry, Remote Sensing and Spatial Information Sciences. Vol. XXXVII. Part B5.
- Moumen, T., et al, 2003, “Nonmetric Lens Distortion Calibration: Closed-form Solutions, Robust Estimation and Model Selection” IEEE International Conference on Computer Vision Vol. 2.
- Nerosky, L. A., 2001, “Medição de Formas Livres Através da Integração de um Sensor Óptico Tipo "Folha de Luz" em um Braço de Medição” Dissertação, PósMCI, UFSC.
- Nister, D. et al, 2004, “Visual Odometry” In Proc. IEEE Computer Society Conference on Computer Vision and Pattern Recognition (CVPR) pages 652-659.

- Pinto T. L., et al, 2009 “Optical measurement and color map projection system to highlight geometrical features on free form surfaces” FRINGE 2009 - The 6th International Workshop on Advanced Optical Metrology, 2009, Nürtingen. Springer-Verlag, 2009. v. 1. p. 497-500.
- Pinto, T. L. F. C. “Medição óptica, comparação e sinalização de superfícies com forma livre de grande extensão” Tese, PósMec, UFSC, 2010.
- Proll, K. P., 2004, “Optische Topometrie mit räumlichen Lichtmodulatoren” Thesis, Institut für Technische Optik der Universität Stuttgart.
- Raguse, K., Wiggenhagen, M., 2003, “Quality Parameters of the Optical Data Channel used in Impact Tests” Optical Photogrammetry and Geodesy, Band II. Zürich, 252-258.
- Rautenberg, U., Wiggenhagen, M., 2002 “Abnahme und Überwachung photogrammetrischer Messsysteme nach VDI-2634| Photogrammetrie Fernerkundung Geoinformation, No. 2, pp. 117-124.
- Reich, C., 2000, “3-D shape measurement of complex objects by combining photogrammetry and fringe projection” SPIE, Society of Photo-Optical Instrumentation Engineers, Opt. Eng. 39(1) 224–231.
- Remondino, F., Fraser, C., 2006, “Digital Camera Calibration Methods: Considerations And Comparisons” ISPRS Commission V Symposium 'Image Engineering and Vision Metrology', IAPRS Volume XXXVI, Part 5, Dresden.
- Sen, P., et al, 2005, “Dual Photography” ACM SIGGRAPH.
- Sitnik, R. et al, 2002, “Digital fringe projection system for large-volume 360-deg shape measurement” Optical Engineering, Vol. 41, No. 2.
- Stivanello, M. E., 2008, “Desenvolvimento de uma biblioteca para sistemas de visão estereoscópica para robótica movei” Dissertação, PPGEEL, UFSC.
- Strobl, K. H. et al, 2009, “The Self-Referenced DLR 3D-Modeler” IEEE/RSJ International Conference on Intelligent Robots and Systems.
- Sünderhauf, N. Protzel, P., 2006, “Towards Using Sparse Bundle Adjustment for Robust Stereo Odometry in Outdoor Terrain” In Proc. of Towards Autonomous Robotic Systems, TAROS2006, UK, pp 206-213.
- Tina, Y., et al, 1996, “Comparison of Approaches to Egomotion Computation” Stanford University CA 94305, CVPR, pp. 315--320.
- Triggs, B et al, 2000, “Bundle adjustment – A modern synthesis” Vision Algorithms’99 LNCS, 2000.
- Vassalo, R. F., et al, 2007, “Aprendizagem por Imitação Através de Mapeamento Visuomotor Baseado em Imagens Omnidirecionais” Revista Controle & Automação, Vol.18 no.1.
- VDI/VDE 2634 Part 1, 2002, “Optical 3D measuring systems – Imaging systems with point-by-point probing” VDI/VDE Gesellschaft Mess- und Automatisierungstechnik (GMA), Verein Deutscher Ingenieure, Düsseldorf.
- VDI/VDE 2634 Part 2, 2002, “Optical 3D measuring systems – Optical systems based on area scanning” VDI/VDE Gesellschaft Mess- und Automatisierungstechnik (GMA), Verein Deutscher Ingenieure, Düsseldorf.
- Weng, J. et al, 1992, “Camera Calibration with Distortion Models and Accuracy Evaluation” IEEE Transactions on Pattern Analysis and Machine Intelligence, Vol. 14, N. 10.
- Xiaoling, Z., 2005, “Calibration of a fringe projection profilometry system using virtual phase calibrating model planes” Journal Of Optics A: Pure And Applied Optics 7, 192–197.
- Zhang, S. et al, 2006, “Novel method for structured light system calibration” Optical Engineering 45(8), 083601.
- Zhang, Z., 1998 “A Flexible New Technique for Camera Calibration” Technical Report MSR-TR-98-71, Microsoft Corporation.
- Zhang, Z., 1999 “Flexible Camera Calibration By Viewing a Plane From Unknown Orientations” Computer Vision, The Proceedings of the Seventh IEEE International Conference on, Vol. 1, pp. 666-673.

8. RESPONSIBILITY NOTICE

The authors are the only responsible for the printed material included in this paper.